NANO LETTERS

2003
Vol. 3, No. 7
973−977

Direct Electrodeposition of Highly Dense 50 nm $Bi_2Te_{3-y}Se_y$ Nanowire Arrays

Marisol Martín-González,*,†,‖ G. Jeffrey Snyder,‡ Amy L. Prieto,†,⊥ Ronald Gronsky,§ Timothy Sands,§,# and Angelica M. Stacy†

Department of Chemistry, University of California, Berkeley, Berkeley, California, 94720, Thermoelectric Materials and Devices Team, Jet Propulsion Laboratory, California Institute of Technology, 4800 Oak Grove Drive, Pasadena, California, 91109, and Department of Materials Science & Engineering, University of California, Berkeley, Berkeley, California, 94720

Received February 11, 2003; Revised Manuscript Received April 22, 2003

ABSTRACT

Films and arrays of 200 and 50 nm diameter wires of $Bi_2Te_{3-x}Se_x$ have been electrodeposited in the following general reaction: $2Bi^{3+} + (3-y)HTeO_2^+ + (y)H_2SeO_3 + (9+y)H^+ + 18e^- \rightarrow Bi_2Te_{3-y}Se_y + (6+y)H_2O$. Films produced from an electrolyte of 0.0075 M Bi, 0.0090 M Te, and 0.0010 M Se in 1 M HNO_3 at a potential of ~0 V vs Ag/AgCl are single phase with composition $Bi_2Te_{2.6}Se_{0.4}$ as determined by X-ray diffraction, energy-dispersive X-ray spectroscopy, and scanning electron microscopy. Similar conditions yield arrays of 200 and 50 nm $Bi_2Te_{3-y}Se_y$ wires when deposited into porous alumina templates. The wires are single phase, crystalline, and textured, with up to 85% pore filling.

Introduction. Thermoelectric materials are attracting renewed interest because of the promise that low-dimensional, or quantum-confined, systems will have greater efficiencies compared with bulk materials.[1] If the thermoelectric efficiencies are improved by a factor of ~3, then thermoelectric coolers and power generators will become competitive with conventional compressor-based refrigerators and power sources.[2] Good target materials for thermoelectric nanowires are Bi_2Te_3 derived alloys, $Bi_2Te_{3-y}Se_y$ (n-type) and $Bi_{2-x}Sb_xTe_3$ (p-type). These are currently the most efficient thermoelectric materials at 25 °C in bulk form. Prior work has shown that high quality arrays of Bi_2Te_3 nanowires can be obtained by electrodeposition into porous alumina templates.[3] Since a working thermoelectric device consists of n-type and p-type legs assembled thermally in parallel and electrically in series, the critical next step is the preparation of n- and p-type materials. In this paper, we report the electrochemical synthesis of wire arrays in porous alumina of n-type $Bi_2Te_{3-y}Se_y$ with $y \sim 0.3$. This composition is the one that is optimal for bulk thermoelectric applications of $Bi_2Te_{3-y}Se_y$.[2]

Prior work has shown that Bi_2Te_3 can be deposited directly by electrochemical reduction of $HTeO_2^+$ from acidic aqueous solutions in the presence of Bi^{3+}.[3−5] By attaching a porous alumina template to a conducting material, the growth of Bi_2Te_3 can be confined by the pore walls. Since the deposition occurs by electron transfer from the surface of the conducting material, Bi_2Te_3 nucleates at the bottom of the pores and grows continuously up the pore. Several desirable characteristics of the materials produced by this method are that the wires are continuous, the pore densities (~7×10^{10} pores/cm^2) and aspect ratios (up to ~1000) are high, and the pore dimensions are tunable over a wide range of diameters (~7 nm to 300 nm) and lengths (to >100 μm).[6] There has been a previous report on the preparation of films of $Bi_2Te_{3-y}Se_y$ ($y = 0.05$).[7] We have therefore extended prior work to fabricate 200 and 50 nm wire arrays of the ternary $Bi_2Te_{3-y}Se_y$ alloy. The 50 nm diameter wires are small enough to anticipate phonon-dampening effects, which should lead to an enhanced thermoelectric Figure of Merit.[2,8−11,15]

Experimental Section. Solutions of Bi^{3+} (7.5×10^{-3} M) plus (a) $HTeO_2^+$ (9×10^{-3} M) and H_2SeO_3 (1×10^{-3} M); (b) $HTeO_2^+$ (8×10^{-3} M) and H_2SeO_3 (2×10^{-3} M); and (c) $HTeO_2^+$ (1×10^{-2} M) in 1 M HNO_3 were studied. Concentrated nitric acid (Fisher, 69.1%) was used to dissolve elemental Bi (Mallinckrodt, 99.8%), Se (Stream Chemicals, 99.99%), and Te (Alfa Aesar, 99.9998%), and the solution was subsequently diluted to 1 M HNO_3. Solutions (a) and (b) were used to prepare films, and 200 and 50 nm wire

* Corresponding author: marisol@icmm.cnm.csic.es, msmg@ole.com
† Department of Chemistry, UC, Berkeley.
‡ California Institute of Technology.
§ Department of Materials Science & Engineering, UC, Berkeley.
‖ Current address: Instituto de Microelectrónica de Madrid, IMM (CNM-CSIC) C/ Isaac Newton, 8 (PTM) 28760 − Tres Cantos. Madrid (Spain). E-mail: marisol@imm.cnm.csic.es.
⊥ Current address: Department of Chemistry and Chemical Biology, Harvard University, 12 Oxford Street Cambridge, MA 02138.
Current address: School of Materials Engineering, School of Electrical and Computer Engineering, and the Birck Nanotechnology Center, Purdue University, 501 Northwestern Ave., West Lafayette, IN 47907-2036.

10.1021/nl034079s CCC: $25.00
Published on Web 05/23/2003

arrays. The 200 nm templates were purchased from Whatman and the 50 nm porous alumina templates were prepared as described previously.[3]

Cyclic voltammograms were recorded with a Bioanalytical Systems Basomatic CV50W unit. A three-electrode electrochemical cell was employed consisting of a Ag/AgCl reference electrode (3M NaCl, 0.175 V vs NHE), a Pt disk working electrode, and a Pt wire counter electrode. The working electrode was polished and ultrasonically cleaned before each voltammogram in order to ensure a clean surface for each scan. Voltammograms were recorded at different scan rates (between 1 and 50 mV/s) and multiple scans were done for each scan rate. Typical scans performed at 10 mV/s are shown for comparative purposes in this paper. The potential limits for the voltammograms were established by scanning first from 2 to −2 V to determine the solvent window and the oxidation−reduction potentials.[5]

Electrodeposition of $Bi_2Te_{3-y}Se_y$ was performed using a standard three-electrode cell (EG&G PAR model 273 potentiostat/galvanostat). The working electrode was a 1 cm diameter 200 nm porous alumina filter obtained from Whatman or a homemade template with a Pt layer sputter deposited on one side (RANDEX, Perkin-Elmer model 2400). The alumina template was then glued with Ag paint to a Cu wire. The back of the composite was insulated with clear nail polish to ensure that deposition could occur only at the base of the pores. The counter electrode was Pt gauze attached to a Pt wire and the reference electrode was the same as above. The volume of the electrolytic bath was 50 mL and the temperature was 25 °C for all depositions. Depositions of $Bi_2Te_{3-y}Se_y$ were performed under potentiostatic control with potentials $-0.1\ V < E < +0.1\ V$ vs Ag/AgCl using solutions (a) and (b), see top of the section.

The composition and morphology of the films and nanowire arrays were analyzed using several techniques: energy dispersive spectroscopy (in both a JEOL 6300 SEM and a JEOL 200CX TEM); X-ray diffraction (Siemens D5000, Cu Kα radiation, 40 kV, 30 mA); and field emission scanning electron microscopy (FESEM, Hitachi S-5000). Energy dispersive spectroscopy (EDS) was used to determine the chemical composition of the film and nanowires. In a typical EDS measurement on a film, the composition was measured at 5 points along the length of the cross section of the film. The standard deviations of the measurements were within 3 atomic %, which is typical for samples with such surface roughness. To prepare specimens for study by SEM, the Pt layer was removed by mechanically polishing on a Buehler Ecomet 3 variable speed grinder/polisher using a colloidal SiO_2 dispersion (diameter ∼50 nm, Allied) on a Buehler polishing microcloth and soaked for several hours to eliminate the polishing remains from the surface. For 200 and 50 nm wire arrays, lattice parameters and chemical compositions were calculated from diffraction peak shifts relative to the peak positions for the binary Bi_2Te_3 using the Pt substrate as an internal standard, and by EDS of single nanowires in the TEM. For the TEM study, a 45 g/L CrO_3 in 3.5 vol % H_3PO_4 solution was used to selectively dissolve the alumina template for approximately 1 day, followed by replacing the etching solution with isopropyl alcohol through a series of dilutions, and then dispersing the remaining individual wires onto a TEM grid. Field emission scanning electron microscopy was carried out to determine the morphology and grain size of the electrodeposited thin films and of the 200 and 50 nm nanowire arrays.

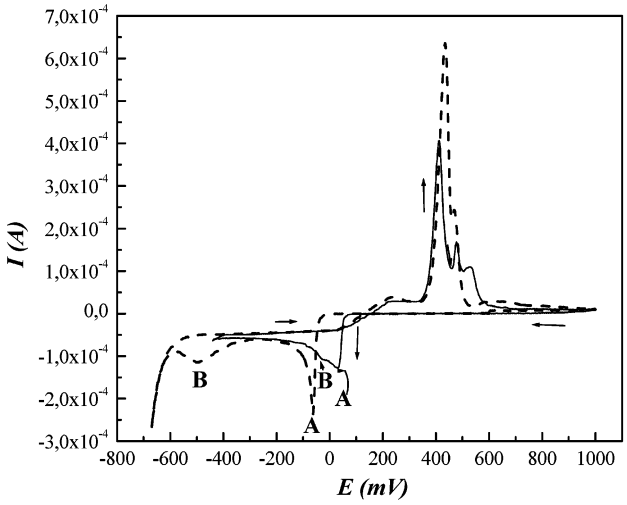

Figure 1. Cyclic voltammetry scans. Solutions of Bi^{3+} (7.5×10^{-3} M) plus (−) $HTeO_2^+$ (9×10^{-3} M), and H_2SeO_3 (1×10^{-3} M) and (- - -) $HTeO_2^+$ (1×10^{-2} M) in 1 M HNO_3. Scan rate = 0.01 Vs^{-1}, reference electrode = Ag/AgCl (3 M NaCl), temperature = 25 °C. A and B correspond to the two reduction peaks for each compound.

Results and Discussion. Cyclic voltammograms for solutions with and without H_2SeO_3 are compared in Figure 1. The overall reaction responsible for the deposition can be described as

$$2Bi^{3+} + (3-y)HTeO_2^+ + (y)H_2SeO_3 + (9+y)H^+ + 18e^- \rightarrow Bi_2Te_{3-y}Se_y + (6+y)H_2O \quad (1)$$

Note: $HTeO_2^+$ and H_2SeO_3 are the stable species for $Te^{4+}_{(aq)}$ and $Se^{4+}_{(aq)}$ at pH = 0, according to the E-pH Pourbaix diagram.[12]

The reduction processes for electrolytes containing H_2SeO_3 (−) are comparable to those without H_2SeO_3 (- - -). There are two reduction processes in both cases, indicating two different mechanisms for the deposition of $Bi_2Te_{3-y}Se_y$, as has been reported previously for Bi_2Te_3.[5] For solutions with Se, $Te_{1-x}Se_x$ alloys are formed instead of elemental Te.[5] The shift of the reduction potentials to more positive values upon addition of H_2SeO_3 is consistent with previous reports that the deposition of Bi_2Se_3 occurs at more positive potentials compared with Bi_2Te_3.[13] The observation of a reduction potential between Bi_2Te_3 and Bi_2Se_3 implies formation of a single phase with a reduction potential that is between the reduction potentials of the binary alloys.

To test the hypothesis of the direct formation of the compound, films were electrodeposited to examine the composition, homogeneity, and crystallinity of the deposited material. When the potential was held more negative than ∼0 V vs Ag/AgCl, a dark deposit was observed on the Pt

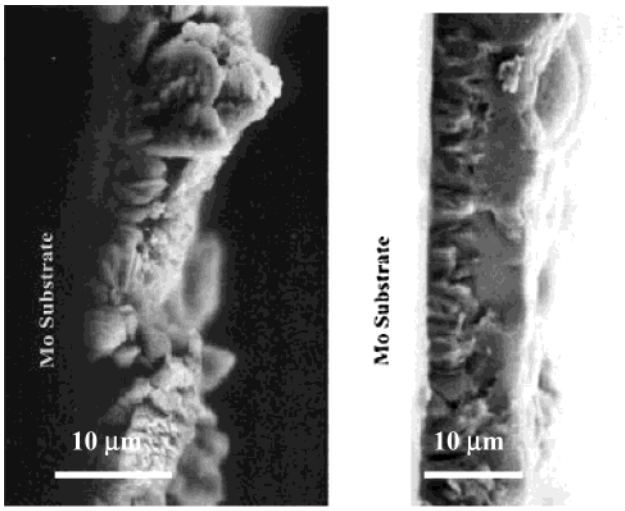

Figure 2. Cross section of two different films on Mo sheet: (a) ~10 μm $Bi_{2.1}Te_{2.6}Se_{0.3}$ black in color, rapid growth conditions, and (b) ~10 μm $Bi_2Te_{2.4}Se_{0.6}$ gray in color, slower growth conditions. The depositions were carried out at $E \sim -0.1$ V vs Ag/AgCl (3M NaCl).

electrode. Energy dispersive spectroscopy (EDS) analysis of films deposited at −0.1 V vs Ag/AgCl confirmed the substitution of about 13% of the Te by Se. This could mean that Se has substituted for Te and one phase has formed, or that the film is a mixture of Bi_2Te_3 and Bi_2Se_3. All maxima in the powder X-ray diffraction pattern (XRD) for the deposits could be indexed to the rhombohedral space group, $R\bar{3}m$, for the Bi_2Te_3 structure-type, indicating that a single phase had formed. The peaks are shifted to smaller *d* spacings compared to pure Bi_2Te_3 and fall roughly in the middle of those observed for Bi_2Te_3 (PDF 15−0863; $a = 4.385$ Å, $c = 30.48$ Å) and Bi_2Te_2Se (PDF 29−0247; $a = 4.240$ Å, $c = 29.66$ Å). Taken together, the EDS and XRD results confirmed the electrodeposition of a single phase and indicated an approximate composition of $Bi_2Te_{2.6}Se_{0.4}$. This is close to the level of Se substitution of 10−16% in Bi_2Te_3 for the n-type leg used in thermoelectric devices.[2]

To determine that the dominant carriers for $Bi_2Te_{3-y}Se_y$ films are in fact electrons, the Seebeck coefficient was measured at room temperature. For these measurements $Bi_2Te_{3-y}Se_y$ films were electrodeposited onto a conducting sheet (Mo). Two different kinds of samples were prepared for comparison. Sample I (a cross section is shown in Figure 2a) was grown under fast conditions using solution (a). The composition of the sample was found to be $Bi_{2.1}Te_{2.6}Se_{0.3}$ as determined by EDS and its color was black. Sample II (cross section shown in Figure 2b) was grown under slower growth conditions using solution (b). The composition of the sample was determined to be $Bi_2Te_{2.4}Se_{0.6}$ by EDS and it was gray. The Seebeck coefficients of as-deposited films were inhomogeneous across the films with values ranging from −10 to −55 μV/K near room temperature for both films in contrast to that expected (−180 to −200 μV/K) from bulk material with the same sample composition and crystal structure. Heating the films (both samples I and II) at 250 °C in forming gas for 2 h yielded Seebeck values that were more homogeneous across each film, with Seebeck coefficients ranging from −40 to −55 μV/K near room temperature. These values are in good agreement with those reported previously for n-type Bi_2Te_3 electrodeposited films.[14] Considering that Se substitution for Te generally reduces the magnitude of the Seebeck coefficient in bulk material,[15] the results for the alloy films are encouraging. As can also be seen in Figure 2a and 2b, slower growth conditions give smoother and denser films, although more time is needed to achieve the same film thickness (~10 μm); 3 vs 5 h, respectively.

Wire arrays with 200 nm diameters were prepared using commercially available porous alumina. Pt was sputtered onto one side of the alumina, and the alumina/Pt composite was used as the working electrode. Note that Pt was used instead of Ag (as it had been used in previous work for deposition of host Bi_2Te_3)[3] because Se reacts with Ag. The conditions for the deposition of films were used successfully for deposition into the 200 nm porous alumina templates. The templates became uniformly gray in color during deposition, when slower growth conditions were used. The deposition was allowed to continue for about 22 h until an increase in the current was observed, indicating that some of the pores were filled and deposition was now occurring on the top surface. The composition of the deposit on the top surface as determined by EDS was $Bi_{2.1}Te_{2.4}Se_{0.5}$, similar to that observed for films. Note that no cross-section compositional analysis can be done for phases with Se within an alumina template since the Se L line overlaps with the Al Kα line in an EDS spectrum and the amount of Se in the wire is small compared with the amount of Al from the template. In previous work with Bi−Sb phases, we determined that the composition on the surface is not the same as in the wires. Since EDS on the SEM seems to provide information that is consistent with other measurements (e.g., XRD), and since it is interesting to know the homogeneity of the composition along the length of the wire, single-wire measurements were done in a TEM in order to elucidate both the composition and the homogeneity of the composition along the wires. The alumina was selectively etched using a CrO_3/H_3PO_4 bath to free the $Bi_2Te_{3-y}Se_y$ wires in solution. After dispersing droplets of the solution on a transmission electron microscope grid, the composition along the length of the wire was analyzed by EDS, confirming a composition of $Bi_2Te_{2.5}Se_{0.5}$.

After polishing the excess film off the top surface, SEM images revealed that ~75% of the pores were filled. Cross-sectional images, Figure 3, show that the individual wires were continuous and dense, ~200 nm in diameter and ~20 μm long (an aspect ratio of 100), resulting from a deposition rate that was very slow (~0.9 μm/h). The individual wires filled the pores, and the sides and edges were smooth. The XRD patterns for the 200 nm wire arrays were similar to those described above for films, indicating that the wires were polycrystalline and single phase with a composition determined by XRD to be $Bi_2Te_{2.5}Se_{0.5}$. It is notable that the 110, 205, and 125 peaks are higher in intensity than expected for a random polycrystalline sample (see Figure 4). The very high intensity of the 110 peak relative to the 015 peak (more

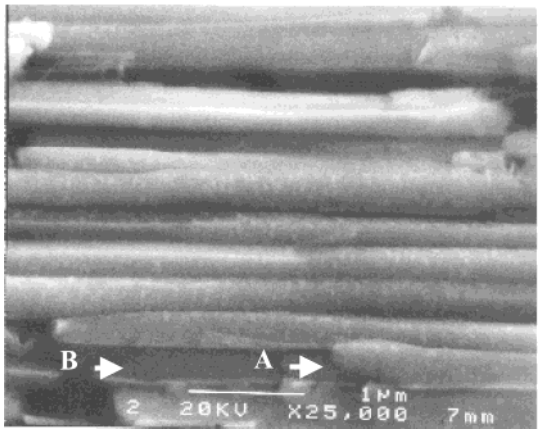

Figure 3. Cross-section of 200 nm $Bi_{2.1}Te_{2.4}Se_{0.5}$ wire array. The wires are continuous, dense, and ~20 μm long. The depositions were carried out at $E \sim 0$ V vs Ag/AgCl (3 M NaCl) for 20 h. Arrows: A indicates the 200 nm $Bi_{2.1}Te_{2.4}Se_{0.5}$ wires and B the alumina template.

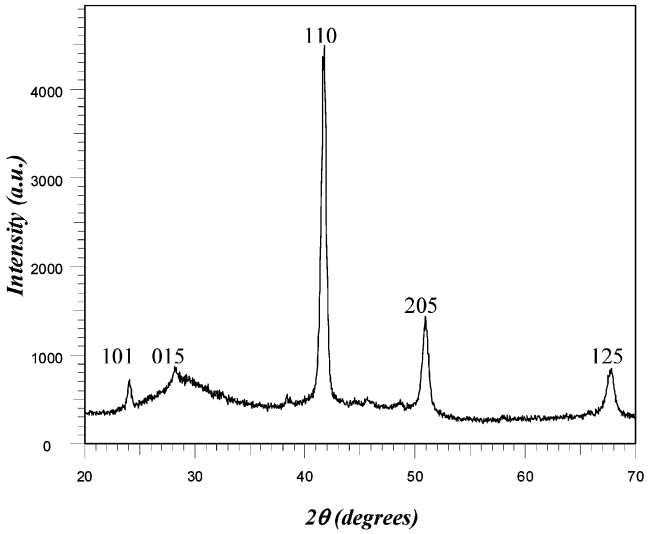

Figure 4. XRD pattern of 200 nm $Bi_{2.1}Te_{2.4}Se_{0.5}$ wire array. The deposition was carried out at $E \sim 0$ V vs Ag/AgCl (3 M NaCl) for 20 h.

intense for a polycrystalline sample) is due to preferred orientation, indicating that the wires are textured along [110]. There is a broad low angle bulge due to the amorphous Al_2O_3 template, and the wires are highly crystalline as confirmed by the bright field/dark field TEM images shown in Figure 5.

Obtaining high quality 50 nm wire arrays was significantly more difficult.[3] The templates must be free of cracks or the deposition will occur preferentially into the crack rather than the smaller diameter pores. We have fabricated the templates using a procedure published previously.[3,16] In addition, the electrochemical processes are altered at the small pore sizes because of changes in diffusion rates to the electrode surface at the base of the pores. This slows down the deposition process below the rate obtainable for films or for larger, 200 nm pore, templates. It took approximately 20 h to fill 25 μm of a 60 μm thick template with 50 nm pores, at 2 °C and at ~+0.1 V vs Ag/AgCl. The current density was ~1 mA/cm^2 and the solution conditions were the same as those

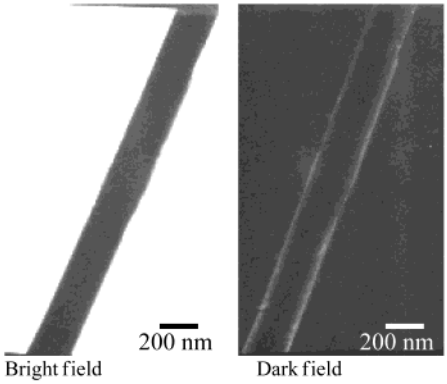

Figure 5. A single $Bi_{2.1}Te_{2.4}Se_{0.5}$ wire with a diameter of ~200 nm. Bright field/dark field pair shows that the wires are highly crystalline.

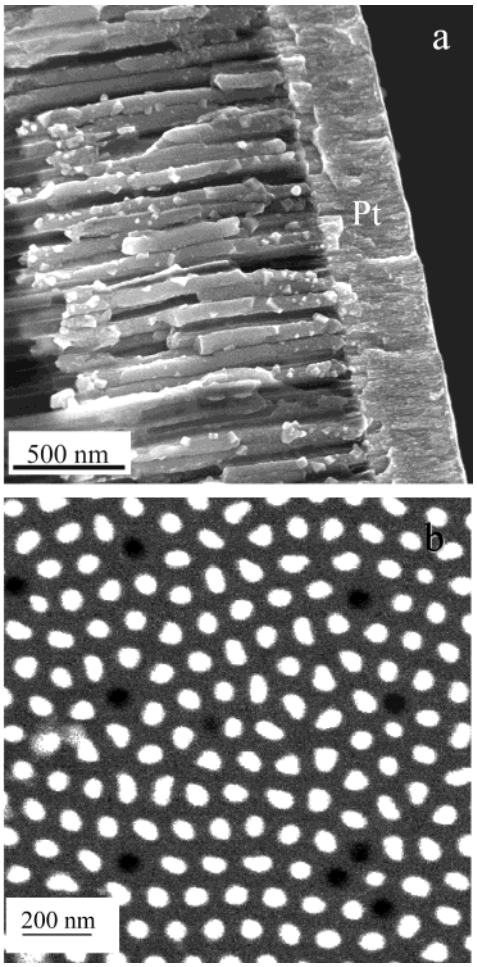

Figure 6. SEM of 50 nm $Bi_2Te_{3-y}Se_y$ nanowire arrays: (a) cross section using secondary electrons and (b) bottom view after removal of the Pt electrode by mechanical polishing using backscattering electrons. The electrodeposition conditions of these images were carried out at $E \sim +0.1$ V vs Ag/AgCl (3 M NaCl) for 15 h.

used for 200 nm arrays and films. However, the slower growth rate also increases the wire quality, yielding higher crystallinity and improved compositional homogeneity. It is interesting to note that by reducing the pore size, the effective potentials became more positive or less negative (0 V vs +0.1 V vs Ag/AgCl for 200 and 50 nm, respectively).

The 50 nm templates became gray in color during deposition, although it took more time than for comparable experiments on binary Bi_2Te_3 alloys. X-ray diffraction patterns are similar to those obtained for the films and 200 nm wire arrays, although the signal-to-background ratio is smaller because there is less material present in the 50 nm template. The XRD patterns indicate that the samples are polycrystalline and single phase with a composition between that of Bi_2Te_3 and Bi_2Te_2Se, similar to the films and 200 nm wires. SEM images in cross-sectional view using secondary electrons indicate that the individual wires are continuous and very dense, as shown in Figure 6a. The individual 50 nm wires fill the pores and the wire edges are relatively smooth. A backscattering SEM image of the bottom of the template after removal of the Pt by mechanical polishing (see Figure 6b) reveals regions with good pore filling (∼85%) in which the wires are fairly uniform in diameter.

Conclusions. We conclude that electrodeposition at potentials near 0 V vs Ag/AgCl from a solution of Bi^{3+} and $HTeO_2^+$ in 1.0 M HNO_3 to which H_2SeO_3 has been added yields films and wires of $Bi_2Te_{3-y}Se_y$. The films and wires are single phase and crystalline, and the wires are dense, highly crystalline, continuous, and uniform. The very slow deposition rate produces not only high quality nanowires but also uniform nanowire lengths across the template. The high degree of pore filling yields a high wire density as is necessary to carry the current for the n-type leg in thermoelectric devices.

Acknowledgment. This work was funded by the Office of Naval Research under grant number N00014-01-1-1058. Additional support was provided by a Department of Defense ONR-MURI on Thermoelectrics grant, number N00014-97-1-0516. M.S.M.G thanks MEC/Fulbright for a postdoctoral fellowship and A.L.P. thanks Lucent Technologies, Bell Labs for a CRFP fellowship. The authors also thank Prof. Jeffrey Long and his group for the use of the Bioanalytical Systems Basomatic CV50W, Mr. Ron Wilson, MSE/UCB, and Dr. Tamara Radetic, NCEM/ LBNL, for their help with EDS-SEM and EDS-TEM, respectively; Dr. Gordon Vrdoljak, CNR/UCB, for assistance with the field emission SEM, and the Campus Electron Microscope lab and EECS Microfabrication Laboratory for research facilities.

References

(1) Hicks, L. D.; Dresselhaus, M. S. *Phys. Rev. B* **1993**, *47*, 12727. (b) Harman, T. C.; Taylor, P. J.; Spears, D. L.; Walsh, M. P. J. *Electron. Mater.* **2000**, *29*, L1. (c) Venkatasubramanian, R.; Siivola, E.; Colpitts, T.; O'Quinn, B. *Nature* **2001**, 413. (d) Cho, S. DiVenere, A.; Wong, G. K.; Ketterson, J. B.; Meyer, J. R. *Phys. Rev. B: Condens. Matter* **1999**, *59*, 10691. (e) Broido, D. A.; Reinecke, T. L. *Appl. Phys. Lett.* **1995**, *67*, 100.

(2) CRC Handbook of Thermoelectrics; Rowe, D. M., Ed.: CRC Press: Boca Raton, 1995.

(3) Prieto, A. L.; Sander, M. S.; Martín-González, M. S.; Gronsky, R.; Sands, T.; Stacy, A. M. *J. Am. Chem. Soc.* **2001**, *123*, 7160. (b) Sapp, S. A.; Lakshmi, B. B.; Martin, C. R. *Adv. Mater.* **1999**, *11*, 402. (c) Sander, M. S.; Prieto, A. L.; Gronsky, R.; Sands, T.; Stacy, A. M. *Adv. Mater.* **2002**, *14*, 665.

(4) Takahashi, M.; Oda, Y.; Ogino, T.; Furuta, S. *J. Electrochem. Soc.* **1993**, *140*, 2550. (b) Magri, P.; Boulanger, C.; Lecuire, J. M. In *Electrodeposition of Bi_2Te_3 Films*; Mathiprakasam, B., Heenan, P., Eds.; AIP Press: Kansas City, 1994; p 277. (c) Martin, C. R. *Science* **1994**, *266*, 1961.

(5) Martín-González, M. S.; Prieto, A. L.; Gronsky, R.; Sands, T.; Stacy, A. M. *J. Electrochem. Soc.* **2002**, *149*, C546−C554.

(6) Shingubara, S.; Okino, O.; Sayama, Y.; Sakaue, H.; Takahagi, T. *Jpn. J. Appl. Phys.* **1997**, *36*, 7791.

(7) Fleurial, J.-P.; Borshchevsky, A.; Ryan, M. A.; Phillips, W. M.; Snyder, G. J.; Caillat, T.; Kolawa, E. A.; Herman, J. A.; Mueller, P.; Nicolet, M. MRS 1998 Fall Meeting-Symposium Z, Boston, MA, December 3, 1998; Vol. 545, p 493.

(8) Balandin, A.; Wang, K. L. *Phys. Rev. B− Condens. Matter* **1998**, *58*, 1544.

(9) Balandin, A.; Wang, K. L. *J. Appl. Phys.* **1998**, *84*, 6149.

(10) Dresselhaus, M. S.; Koga, T.; Sun, X.; Cronin, S. B.; Wang, K. L.; Chen, G. *Low Dimemsional Thermoelectrics; Proceedings ICT, Ed.; IEEE* 1997, *16*, 12.

(11) Dresselhaus, M. S.; Dresselhaus, G.; Sun, X.; Zhang, Z.; Cronin, S. B.; Koga, T.; Ying, J. Y. *Microscale Thermophys. Eng.* **1999**, *3*, 89.

(12) Pourbaix, M. J. N. In *Atlas of Electrochemical Equilibria in Aqueous Solution* (English translation, 2nd ed.; Franklin, J. A., Ed.; National Association of Corrosion Engineering: Houston, TX, 1974.

(13) Torane, A. P.; Lokhande, C. D.; Patil, P. S.; Bhosale, C. H. *Mater. Chem. Phys.* **1998**, *55*, 51.

(14) Stoltz, N. G.; Snyder, G. J. *Proceedings of the XXI International Conference on Thermoelectrics. ICT'02*; IEEE: Long Beach, California, 2002; p 28.

(15) Nolas, G.; Sharp, J.; Goldsmid, H. J. In *Principles of Thermoelectrics: Basics and New Materials Development*; Springer Series in Materials Science; Springer: Berlin, 2001; Vol. 45.

(16) Miller, C. Microporous Aluminum Oxide Films at Electrodes; Ph.D. Thesis, University of California, Berkeley, 1987; p 271. (b) Keller, F.; Hunter, M. S.; Robinson, D. L. *J. Electrochem. Soc.* **1953**, *100*, 411. (c) Zhang, Z.; Gekhtman, D.; Dresselhaus, M. S.; Ying, J. Y. *Chem. Mater.* **1999**, *11*, 1659.

NL034079S